Supplemental Figures

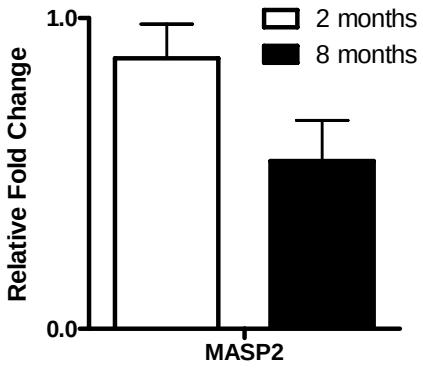

Figure S1. Expression of *MASP2* in dysferlin-deficient skeletal muscle. Real-time quantitative RT-PCR was performed on quadriceps muscles of 2- or 8-month-old dysferlin-null vs. wild-type mice (A-D, n=3). The mRNA levels of the *MASP2* gene were normalized to *Gapdh* mRNA.

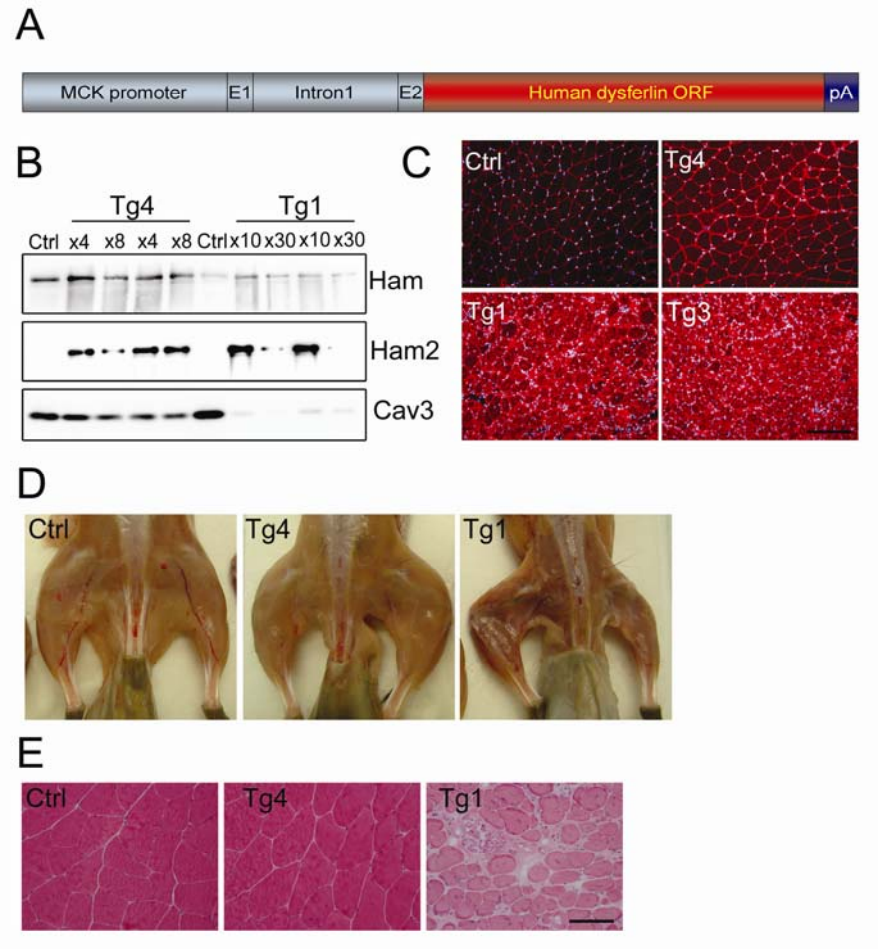

Figure S2. Generation and characterization of muscle-specific dysferlin transgenic mice. (A) Schematic diagram of the dysferlin transgene construct. To drive muscle-specific expression of dysferlin, the 6.5-kb mouse creatine kinase enhancer/promoter was fused to the human dysferlin cDNA followed by SV40 polyadenylation signal sequences. (B) Western blotting analysis of dysferlin expression in two transgenic lines (Tg4 and Tg1). Compared to the endogenous level in control littermates, dysferlin was overexpressed by ~8-fold and ~30-fold in Tg4 and Tg1, respectively. (C) Immunofluorescence staining analysis of muscle sections from the transgenic and control mice. Dysferlin immunofluorescence was increased in the sarcolemma and cytoplasmic punctate vesicles in the Tg4 line, while in the two high expression lines (Tg1 and Tg3), dysferlin was highly increased in the sarcolemma, cytosolic vesicles, but also accumulated in cytosolic aggregates. (D) Gross effect of dysferlin overexpression in muscle. High level of dysferlin overexpression in Tg1 resulted in severe muscle atrophy, while the low overexpression of dysferlin (Tg4) did not produce visible abnormality. (E) Representative H&E-stained histology of quadriceps muscles from WT, Tg4 and Tg1 mice. Scale bars: 200 μm.

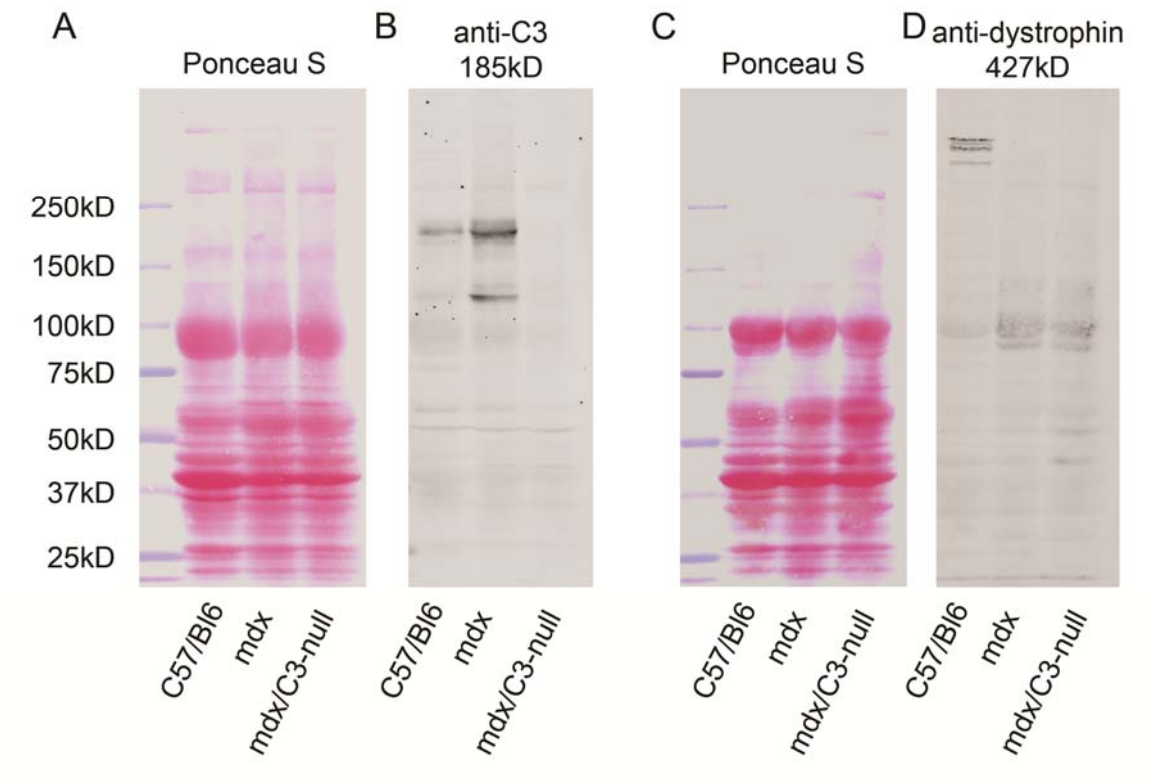

Figure S3. Biochemical characterization of the *mdx*/C3 mice. The total muscle extracts of C57BL/6 (Lane 1), *mdx* (Lane 2) and *mdx*/C3-null (Lane 3) mice were blotted with the anti-C3 antibody (B) and the anti-dystrophin antibody (Mandra-1, D). The Ponceau S staining was performed to demonstrate the equal loading of samples in the different lanes. Note: The samples in C and D were reduced, but not in A and B.

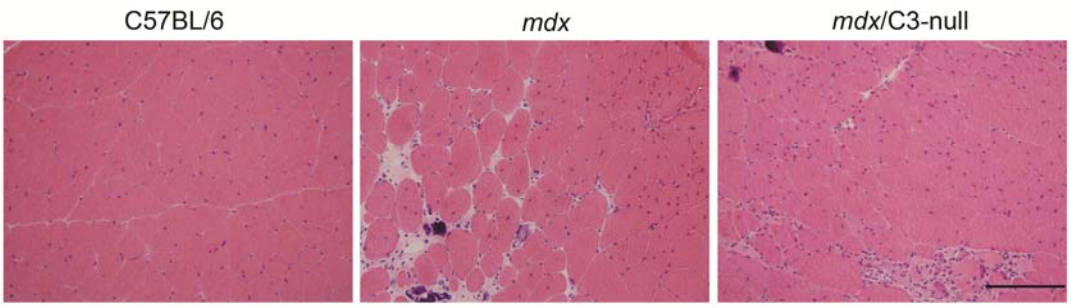

Figure S4. Histological analysis of the *mdx*/C3-null mice. H&E staining of the muscle cryosections from wild-type (WT), *mdx*/C3-null, and *mdx* mice showed that genetic ablation of C3 had not significantly improve the muscle pathology in *mdx* mice. Scale bar: 200 μm.

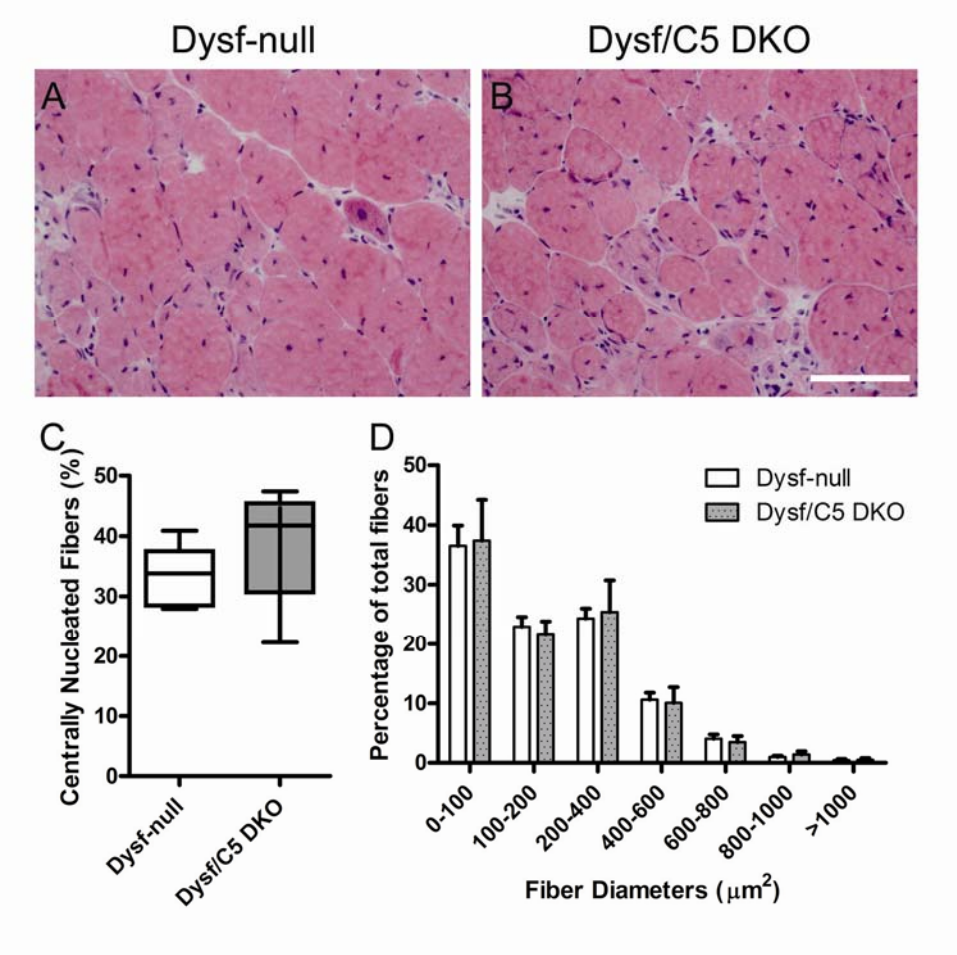

Figure S5. Effect of genetic ablation of complement factor C5 on muscle pathology in dysferlin-deficient mice. (A, B) Representative H&E-stained histology of quadriceps muscles from Dysf-null (A) and Dysf/C5 double-null littermate (B) at 23 weeks old. Scale bars: 100 μm. (C) Fiber areas (grouped into size ranges) from quadriceps muscles of 23-week-old Dysf/C5 double-null mice (N=5). (D) Percentage of fibers containing central nuclei in the quadriceps muscles of 23-week-old Dysf/C5 double-null mice (N=5). The Dysf-null data in C and D were re-plotted from **Figure 7** E and F, respectively.

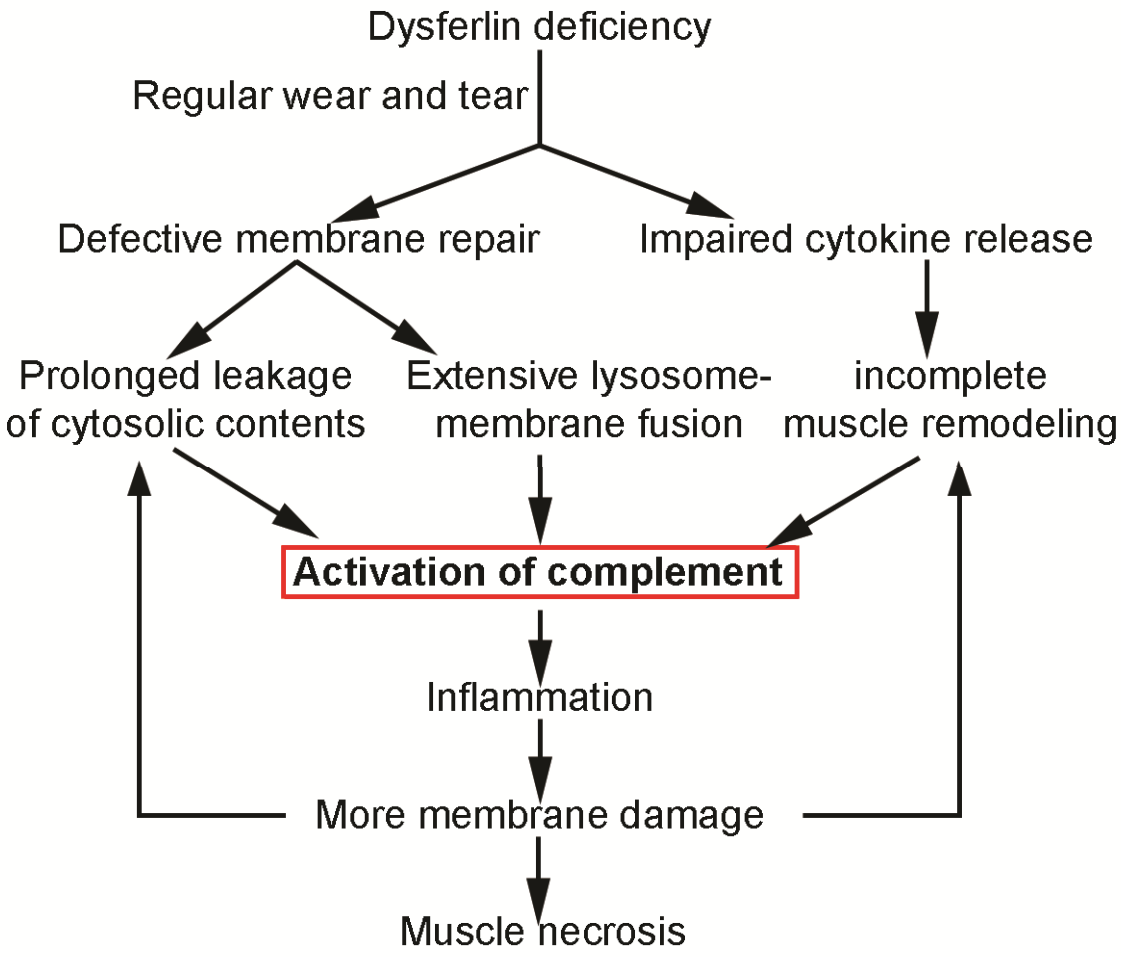

Figure S6. Hypothetical mechanisms linking dysferlin deficiency with activation of the complement system in muscle. Dysferlin deficiency causes defective membrane repair and impaired cytokine release. During regular muscle wear and tear, defective dysferlin-mediated membrane repair results in prolonged leakage of cytosolic conentents and extensive lysosome-mediated membrane fusion may occur; while impaired cytokine release may account for delayed recruitment of neutrophils and incomplete muscle remodeling. These events could activate the complement system and cause muscle inflammation, resulting in more membrane damage and eventually leading to muscle necrosis.

Supplemental Methods

Mouse models. Dysferlin-null mice (1) generated in our lab (backcrossed to C57BL/6J for six generations) and consomic dysferlin-null strain C57BL/6J-Chr 6A/J obtained from Jackson laboratory were used in this study. C3-null mice (B6.129S4-C3^{tm1Crr}/J) generated in the laboratory of Dr. Michael C. Carroll (2) were obtained from Jackson laboratory and they were backcrossed to a C57BL/6J background for at least 6 generations. Consomic C5-null mice (C57BL/6J-Chr2$^{A/J}$/NaJ) were purchased from Jackson Laboratory. Other mouse strains obtained from Jackson Laboratories include C57BL/6, *mdx*/C57BL/10ScSn (*mdx*), and SJL/J. The C5-null and C3-null were bred with dysferlin-null mice to generate dysferlin/C5 and dysferlin/C3 double mutant mice. The C3-null mice were bred with *mdx* mice to generate *mdx*/C3-null mice. Identification of mutant or transgenic mice was performed by PCR genotyping of genomic DNA prepared from mouse tail snips. Mice were maintained at the University of Iowa Animal Care Unit in accordance with the institute's animal usage guidelines. All animal studies were authorized by the Animal Care Use and Review Committee of The University of Iowa.

Antibodies. The mouse monoclonal antibodies Hamlet against dysferlin (Novacastra), Mandra-1 against dystrophin (Sigma-Aldrich), macrophage cell marker Mac-1 (University of Iowa Hybridoma Bank), T-lymphocyte marker CD3 (Sigma-Aldrich), B-lymphocyte CD20 (Sigma-Aldrich), caveolin-3 (Transduction Laboratories), C3 (MP Biochemicals), C5b-9 (Abcam, clone aE11), and polyclonal anti-laminin α 2-chain antibody (Alexis) were used for immunoblotting and immunofluorescence analysis. Alexa Fluor 488 or 555-conjugated secondary antibodies were obtained from Invitrogen.

Generation of dysferlin transgenic mice. The full-length human dysferlin cDNA was pieced together from a human cDNA library (a kind gift from Dr. Bento Soares), a clone DKFZp686K20163Q (RZPD, German) and a clone FLJ00175 (Kazusa DNA Research Institute, Japan) and the sequence was confirmed by the University of Iowa DNA Core Facility. The 6.3-kb human dysferlin cDNA was initially ligated into the KpnI site of the pEGFP-C3 vector to form pEGFP-hDysferlin. To drive muscle-specific expression of dysferlin, the 6.5 kb mouse myosin creatine kinase promoter (a kind gift from Jeff Chamberlain) ClaI (blunted)-XhoI fragment was ligated into AatI (blunted)-XhoI sites of pGem7zf followed by an SV40 polyadenylation signal which was PCR engineered with a 5' KpnI site and 3' NotI-SacI linker. The full-length human dysferlin was then cut from pEGFP-hDysferlin with KpnI and inserted into the KpnI site with correct orientation to generate the MCK-dysferlin construct in pGem7zf+. To produce the transgenic mice, the purified EcoRV-NotI 13-kb transgene fragment (Fig. 1) was microinjected into F1 hybrid zygotes from C57BL/6J X SJL/J parents by the University of Iowa Transgenic Animal Facility. The founders bearing a *Dysf*^{im} allele were backcrossed with C57BL/6J mice two to three times. Since SJL mice contain a 171-bp deletion (*Dysf*^{im}) in the dysferlin gene, the founder mice carry one *Dysf*^{im} allele. Therefore, the F1 mice were also screened for *Dysf*^{im} allele using forward and reverse primers 5'- TACAGCTGCTCTGTGGGTGG -3' and 5'- GTGCTGAGAATCAGGGTGGC-3', and any *Dysf*^{im} allele carriers had been removed from the colony.

Contractile properties. Contractile properties were measured in vitro on extensor digitorum longus (EDL) muscles from C57BL/6 and dysferlin-null mice as described

previously(3). Mice were anesthetized by an intraperitoneal injection (I.P.) of 2% avertin (0.0015 ml/g body weight). Supplemental injections were administered to maintain an anesthesia level that prevented responses to tactile stimuli. Intact muscles were removed from each mouse after the mice were euthanized by an overdose of avertin, and the thoracic cavity was opened. Muscles were immersed in an oxygenated bath (95% O_2, 5% CO_2) that contained Ringer's solution (pH 7.4) at 25°C. For each muscle, one tendon was tied securely with a 5-0 suture to a force transducer (one end), and a servo motor (other end). Using twitches with pulse duration of 0.2 ms, the voltage or current of stimulation was increased to achieve a maximum twitch and then increased slightly. Twitches were then used to adjust the muscle length to the optimum length for force development (L_0). The muscle length was set at L_0 , and EDL muscles were stimulated for 300 ms. Stimulation frequency was increased until the force reached a plateau at maximum isometric tetanic force (P_0). The susceptibility to contraction-induced injury was measured during seven identical lengthening contractions each 400 ms long, with the contractions separated by a rest interval of 60 s. Muscles were activated maximally and following a delay of 100 ms, a lengthening ramp of 30% strain (or 40% for the group at 8 months of age) was initiated at a velocity of 1 Lf/s. The muscle was then returned L_o at the same velocity. To assess the force deficit generated by this assay, a measurement of P_0 was made one minute after the last lengthening contraction. Based on measurements of muscle mass, muscle length, fiber length, and P_0, the total fiber cross-sectional area and specific P_0 (kN/m2) were calculated. The data were analyzed by an analysis of variance (ANOVA). When the overall F-ratio for the ANOVA was significant, the differences between individual group means were determined by a single *t*-test. Significance was set *a priori* at $P < 0.05$. Data are expressed as mean ± SEM.

Exercise-activity assay. Mouse housing and exercise-activity rooms were under specific pathogen-free conditions. The exercise-activity assay was performed without anesthesia to avoid the impact of anesthesia on blood glucose and the blood flow to skeletal muscle. Locomotor activity was monitored by using Digiscan Animal Activity Monitoring System running Versamax Windows software (Accuscan Instruments). Mice were tested in individual chambers in sets of 4, for 30 x 1 minute intervals pre- and immediately post-exercise, at the same time every day in the dark, in an isolated room, and with the same handler. Data collected was converted to a Microsoft Excel worksheet and all calculations were done within the Excel program. Animals were mildly exercised using an adjustable variable speed belt treadmill from AccuPacer (AP4M-MGAG, AccuScan Instruments, Inc.), down a 15° grade at 15 mpm for 10 minutes with acclimatization at 3 mpm for 5 minutes.

Membrane repair assay

The membrane repair assay was performed essentially as described (1, 3, 4). Briefly, isolated *flexor digitorum brevis* (FDB) muscle fibers were incubated in the Tyrode solution supplemented with 2.5 μM FM 1-43 (Invitrogen). Membrane damage was induced in the presence of with a 2-photon confocal laser-scanning microscope (Zeiss LCS 510) coupled to a 10-W Argon/Ti:sapphire laser. After initial images were scanned, a 5-μm × 5-μm area of the sarcolemma of the muscle fiber was injury with 1.5-s irradiation at full power. Fluorescence images were captured at 10-second intervals for 5 min after the damage. The fluorescence intensities at the damaged site were quantified by using the ImageJ software (NIH) and plotted against the time after the damage.

Serum Creatine Kinase Assays. Blood for quantitative, kinetic determination of serum creatine kinase activity was collected either after the pre-exercise activity analysis or 2 hours post-exercise by mouse tail vein bleeds, using a Sarstedt microvette CB 300, from non-anesthetized restrained mice. Red cells were pelleted by centrifugation at 10,000 rpm for 4 minutes and serum was separated, collected and analyzed immediately without freezing. Serum creatine kinase assays were performed with an enzyme-coupled assay reagent kit (Stanbio Laboratory) according to manufacturer's instructions. Absorbance at 340 nm was measure every 30 sec for 2 min at 37°C so that changes in enzyme activity could be calculated.

cDNA synthesis and real-time PCR assay. Total RNA was isolated from skeletal muscle using TRIzol reagent (Invitrogen) and suspended in Dnase- Rnase-free distilled water (Invitrogen). First-strand complementary DNA (cDNA) was synthesized from total RNA using the AMV reverse transcriptase (Roche) and random hexamers, according to the manufacturer's instructions. Each of the target genes were real-time amplified from cDNA using oligonucleotides specific to each gene (sequences and conditions available upon request), and *Gapdh* or 28S-RNA was used as the normalization control. cDNA levels were determined using SYBR green in a MyiQ rt-PCR detection system (BioRad). All samples were run in triplicate.

Immunofluorescence analysis. Immunofluorescence staining for dysferlin, caveolin-3 (Cav3), Mac-1, CD3, C3, C5b-9, Lamp-2 was performed on 7 μm transverse muscle cryosections as described previously. For patient biopsies, immunofluorescence staining was

performed on serial cryosections. The anti-dysferlin antibody was purchased from Novocastra.

Fiber area measurement. Caveolin-3 or H&E stained cross sections of quadriceps at the middle belly from 10-week old dysferlin transgenic line 1, 4 and their control littermates were imaged with a Zeiss microscope at 40x magnification. The RGB images were then converted to 8-bit gray images and the fibre area was measured using Image Pro Plus 6 software.

Supplemental References

1. Bansal, D., Miyake, K., Vogel, S.S., Groh, S., Chen, C.C., Williamson, R., McNeil, P.L., and Campbell, K.P. 2003. Defective membrane repair in dysferlin-deficient muscular dystrophy. *Nature* 423:168-172.
2. Wessels, M.R., Butko, P., Ma, M., Warren, H.B., Lage, A.L., and Carroll, M.C. 1995. Studies of group B streptococcal infection in mice deficient in complement component C3 or C4 demonstrate an essential role for complement in both innate and acquired immunity. *Proc Natl Acad Sci U S A* 92:11490-11494.
3. Han, R., Kanagawa, M., Yoshida-Moriguchi, T., Rader, E.P., Ng, R.A., Michele, D.E., Muirhead, D.E., Kunz, S., Moore, S.A., Iannaccone, S.T., et al. 2009. Basal lamina strengthens cell membrane integrity via the laminin G domain-binding motif of alpha-dystroglycan. *Proc Natl Acad Sci U S A* 106:12573-12579.
4. Han, R., Bansal, D., Miyake, K., Muniz, V.P., Weiss, R.M., McNeil, P.L., and Campbell, K.P. 2007. Dysferlin-mediated membrane repair protects the heart from stress-induced left ventricular injury. *J Clin Invest* 117:1805-1813.